ELSEVIER

Journal of Alloys and Compounds 461 (2008) 72–76

Journal of ALLOYS AND COMPOUNDS

www.elsevier.com/locate/jallcom

Hydrogen absorption by Mg_2Ni prepared by polyol reduction

L. Hima Kumar [a], B. Viswanathan [a,*], S. Srinivasa Murthy [b]

[a] *National Centre for Catalysis Research, Department of Chemistry, Indian Institute of Technology Madras, Chennai 600036, India*
[b] *Mechanical Engineering Department, Indian Institute of Technology Madras, Chennai 600036, India*

Received 17 May 2007; accepted 4 July 2007
Available online 19 July 2007

Abstract

Mg_2Ni prepared by polyol reduction method showed that increased hydrogen absorption characteristics. The maximum storage and release capacities are 3.23 and 2.8 wt%, which appears to be encouraging. The electrochemical measurements also support these observations.

Keywords: Hydrogen storage; Polyol reduction; Mg_2Ni; Discharge capacity

1. Introduction

Hydrogen gas storage is one of the important components of hydrogen economy. A variety of materials such as metal, metal alloys, metal hydrides, intermetallics and metal alanates in bulk as well as nano form have been investigated to obtain the desired levels of storage for hydrogen. Magnesium, its alloys and composites constitute an unique and promising materials for hydrogen storage application since these exhibit high hydrogen storage capacity, light weight and low cost. Mg-based intermetallics form hydrides, which are more unstable than MgH_2. The kinetics of hydriding and dehydriding are slow [1]. The hydriding alloys are used as the negative electrode of a rechargeable battery, essentially replacing the cadmium electrode in the widely used Ni–Cd battery, because they have a less detrimental effect on the environment, a high energy density, a higher charge/discharge rate, low temperature capacity and an absence of memory effect [2]. Of all the magnesium-based alloys, Mg_2Ni is one of the most promising material due to its relatively high hydrogen storage capacity (3.8 wt%). However, the reaction of magnesium alloys with hydrogen requires quite high temperatures (573 K) and pressures due to hydriding/dehydriding difficulties. And moreover the polycrystalline Mg_2Ni shows a very low electrochemical discharge capacity (less than 10 mAh/g) [3].

In order to overcome these disadvantages, mechano-chemical preparation of Mg_2Ni was proposed and adopted in almost all studies during the last decade. Its capacity can be improved by employing a mechanical alloying [4–16]. The observed easy activation and improved hydriding kinetics are attributed to the appearance of a nanocrystalline or amorphous state of the material rich in dislocations and special defects and clean and highly reactive surfaces, which lead to an increase of the hydrogen absorption rate. The nanoparticles usually possess unusual electronic and chemical properties, and these make them very different from the bulk materials due to their extremely small particle size and large specific surface area. It was reported that amorphous Mg_2Ni alloy and metallic Ni or Pd composite prepared by mechanical treatment of the Mg_2Ni alloy with Ni or Pd powder, improved greatly the charge/discharge characteristics [17,18]. For the mechanical alloying method, the raw materials are milled by balls made up of iron in order to obtain homogeneous particles. The process results in the introduction of impurities. In addition, this method consumes energy and results in higher cost for the synthesis of alloys.

Hence it is necessary to look for other alternative method to synthesize nanocrystalline alloys. Recently, polyol reduction method has been employed to synthesize a variety of metallic alloy nanoparticles such as Ag–Pd, Co–Ni, Pt–Fe and Mg–Ni [19–22]. The advantage of this method is that it gives the flexibility to synthesize uniform size nanoparticles in desired composition range by adjusting the preparation conditions such as reducing agent, protecting reagent concentration, temperature and reaction time. In the present study, nanosized Mg_2Ni alloy

* Corresponding author. Tel.: +91 44 22574241/5245; fax: +91 44 22574202/5245.
E-mail address: bvnathan@iitm.ac.in (B. Viswanathan).

0925-8388/$ – see front matter © 2007 Elsevier B.V. All rights reserved.
doi:10.1016/j.jallcom.2007.07.028

particles have been synthesized by polyol reduction method followed by annealing. The hydriding/dehydriding kinetics as well as electrochemical characteristics of this material were investigated.

2. Experimental details

2.1. Synthesis of Mg_2Ni alloy

The Mg–Ni alloy in nanoscale was prepared by chemical reduction using polyol process followed by annealing. In a typical procedure, 0.027 mol magnesium acetate (Merck, 99%) and 0.013 mol nickel acetate (Merck, 99%) were dissolved in 150 ml of ethylene glycol (AR grade) with 2:1 mol ratio. Then 10 g of the polyvinylpyrrolidone (PVP) dissolved in 150 ml of ethylene glycol was added and stirred for 30 min. The resulting mixture was refluxed at 453–463 K. When the temperature had reached the set temperature 453 K, the refluxing was continued for an additional 10 min. The $PdCl_2$ (Lancaster, 99%) with 0.001 mol ratio of (Pd/metal) dissolved in 10 ml ethylene glycol was further added and reflux continued for 1 h at the set temperature. Pd acts as a nucleating agent for the growth of nanoparticles of Mg and Ni metals. Then the product was washed with absolute ethanol to remove the PVP and centrifuged at 6000 rpm for several times. The as synthesized Mg–Ni alloy was dried at 343 K in vacuum followed by annealing at 573 K in hydrogen atmosphere for 3 h.

2.2. Characterization

XRD patterns were obtained by a powder diffractometer (XRD—SHIMADZU XD-D1) using a Ni-filtered Cu Kα X-ray radiation. The scan runs was seen in step scan mode with a step interval of 0.1°/s over the 2θ range of 10–80°. The sample was deposited on the carbon coated copper grid by using the ultrasonically dispersed alloy nanoparticles in methanol and transmission electron microscope (TEM) images were recorded by JEOL-JEM 100SX microscope utilizing an acceleration voltage of 100 kV.

2.3. Hydrogen absorption studies

The hydrogen absorption/desorption characteristics were measured using a facility reported earlier [23]. Pressure–composition isotherms were measured separately at 553, 573 and 603 K. Sample mass of 2 g was used for measuring the hydrogen storage properties. Before each measurement the samples were heated to 573 K and evacuated for 3 h.

2.4. Electrochemical studies

The test electrodes were fabricated by pressing mixture of 0.3 g Mg–Ni alloy and Cu powder in a weight ratio of 1:2, into a pellet of 1.3 cm in diameter. Pellet was pasted on glass electrode with Araldite. Subsequently, as current conductor, a copper wire was attached to the pellet by silver paint. Electrochemical measurements were performed using an automatic land battery-testing instrument controlled by a computer. Pt and Hg/HgO were used as the counter electrode and the reference electrode, respectively. In charge–discharge cycle tests, each negative electrode was charged for 12 h at 50 mAg^{-1} and discharged to −0.6 V versus Hg/HgO under different current density in a 6 M KOH aqueous solution. The resting time between charge and discharge was 10 min. The temperature was kept at 300 K.

3. Results and discussion

3.1. Hydrogen sorption studies

Polyol reduction method produces metal/alloy nanoparticles at low temperatures and hence this method is an efficient method alternative to high-energy ball milling. Chia-Ming Chen and Jih-Mirn Jehng [19] prepared Mg–Ni alloys with various Mg/Ni ratios by polyol reduction method. However, the as synthesized material does not transform fully into Mg_2Ni alloy. Therefore it is necessary to anneal the material to facilitate the formation of Mg_2Ni alloy. The X-ray powder diffraction pattern of the Mg–Ni alloy prepared by polyol reduction followed by annealing at 573 K in hydrogen atmosphere for 3 h is shown in Fig. 1. The main reflections are indexable in the hexagonal unit cell of the Mg_2Ni compound (space group P6222). The presence of unreacted Ni is detected by a small reflection at $2\theta = 52.1°$. The broad peaks indicate that the alloy formed by this method was either nanocrystalline or amorphous which is also confirmed by electron microscopy. Fig. 2 presents the TEM image of Mg_2Ni alloy after annealing. TEM image shows the agglomeration of particles and the average particle size of the nanocrystalline Mg_2Ni alloy is in the range of 50 ± 20 nm.

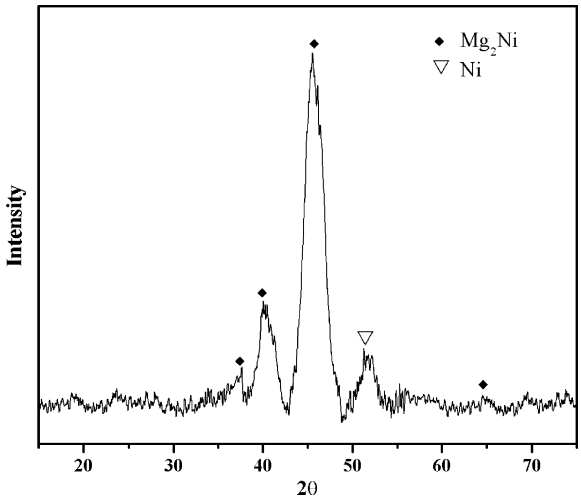

Fig. 1. XRD pattern of Mg_2Ni prepared by polyol reduction followed by annealing at 573 K for 3 h.

Usually the hydrogen absorption properties of Mg_2Ni are very poor. Lot of efforts have been made to improve the kinetics

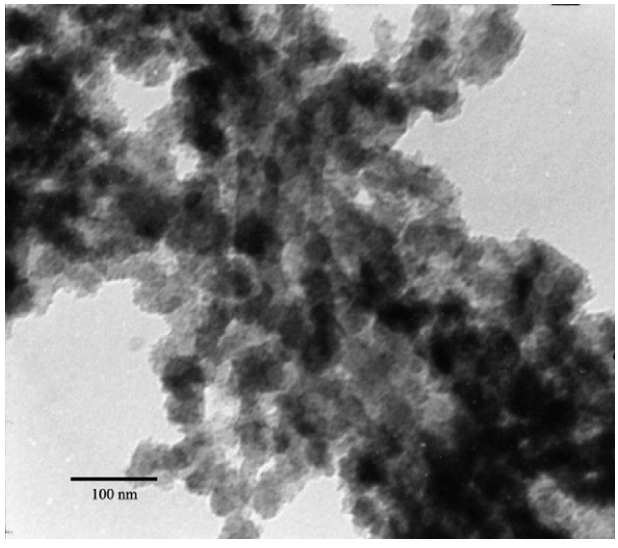

Fig. 2. TEM image of Mg_2Ni prepared by polyol reduction followed by annealing at 573 K for 3 h.

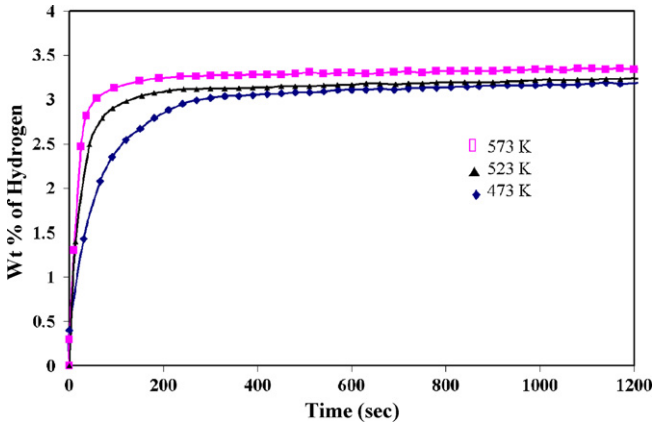

Fig. 3. Kinetic curves of hydriding of nano-Mg_2Ni at an initial pressure of 25 bar and 473, 523 and 573 K.

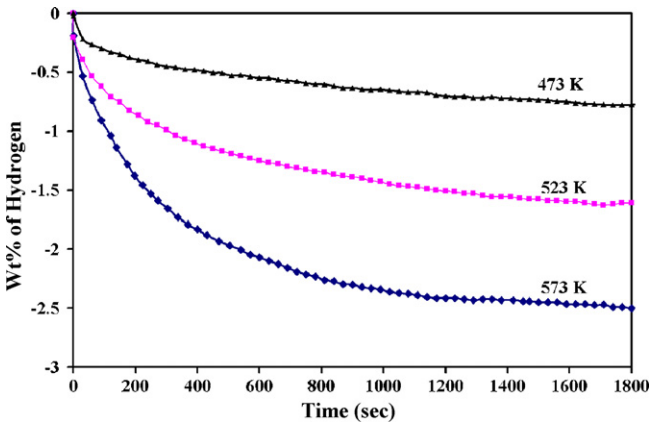

Fig. 4. Hydrogen desorption curves of nano-Mg_2Ni at a pressure of 0.1 bar and 473, 523 and 573 K.

like surface modification, ball milling to induce lattice strain and milling with transition metal/metal oxide catalysts [4–18,24]. The kinetic curves of hydrogen absorption at different temperatures and an initial pressure of 25 bar for the Mg_2Ni prepared by polyol reduction method followed by annealing are shown in Fig. 3. In the case of the polycrystalline Mg_2Ni phase, it was reported that it absorbed/desorbed hydrogen at high temperature (higher than 573 K). However, at a temperature as low as 473 K, the nanocrystalline Mg_2Ni prepared in this study was able to absorb and desorb hydrogen. One can see that the Mg_2Ni compound absorbs hydrogen quickly and reaches maximum with in 1 min at 573 K. The hydrogen absorption curves shown in Fig. 3 are obtained after first hydrogenation dehydrogenation cycle at 573 K. It was worth mentioning that the hydrogen absorption takes place even from first cycle. The hydrogen absorption rate is high due to the smaller size of the Mg_2Ni particles. Since large number of interfaces and grain boundaries are available, the diffusion of hydrogen atoms is easier in the alloy nanoparticles than in the bulk alloys [25]. More over the presence of palladium added during the synthesis of alloy and presence of nickel nanoparticles (shown by the XRD) will facilitate the hydrogen absorption. After 5 min the maximum hydrogen storage capacity of the obtained Mg_2Ni compound is about 3.0, 3.12 and 3.23 wt% at 473, 523 and 573 K, respectively.

The dehydriding kinetic curves for the Mg_2Ni alloy nanoparticles at different temperatures and a pressure of 0.1 bar are presented in Fig. 4. The dehydriding kinetics was measured after the Mg_2Ni was fully hydrogenated at 573 K. As shown in Fig. 5 the material desorbs hydrogen even at 473 K. The rate of desorption is low at lower temperatures and increases with increasing temperature. The maximum amount of hydrogen desorbed was found to be 0.75, 1.61 and 2.5 wt% at 473, 523 and 573 K, respectively in 30 min.

Fig. 5 shows the pressure composition isotherms of Mg_2Ni at 548, 573 and 603 K. Single sloping plateau is observed for absorption/desorption process indicating the presence of nanocrystalline/amorphous nature of the alloy. The slope of plateau decreases with increasing temperature. The plateau with slope indicates that the absorption of hydrogen is by diffusion mechanism as in the case of amorphous or nanocrystalline materials [26]. The slope decrease as the temperature increases may be due to increase in the crystallinity, which reduces the lattice strain and amorphous nature of the alloy. The hydrogen absorption capacities are 2.8, 3.03 and 3.20 wt% at 548, 573 and 603 K, respectively.

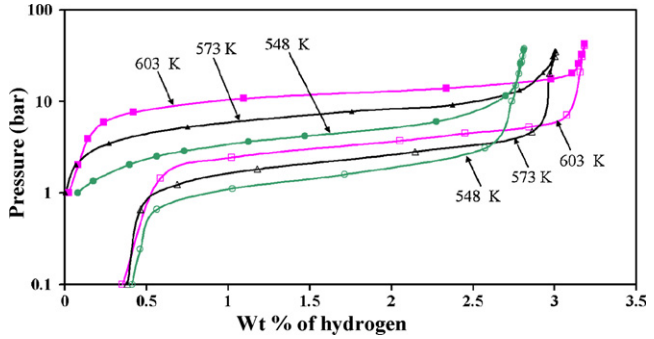

Fig. 5. Pressure–composition isotherms of nano-Mg_2Ni at 548, 573 and 603 K.

The enthalpy (ΔH), and entropy (ΔS) change of hydride formation have been derived by utilizing Van't Hoff plot of $\ln P_{eq}$ versus $1/T$. The Van't Hoff plot for plateau region is shown in Fig. 6. The pressure data were obtained from the midpoint of plateau region from Fig. 5. The parameters, entropy and enthalpy change, were obtained using the least

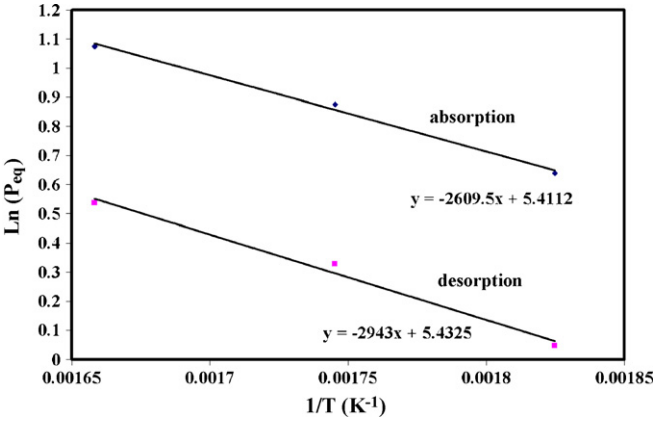

Fig. 6. Van't Hoff plot $\ln P_{eq}$ vs. $1/T$.

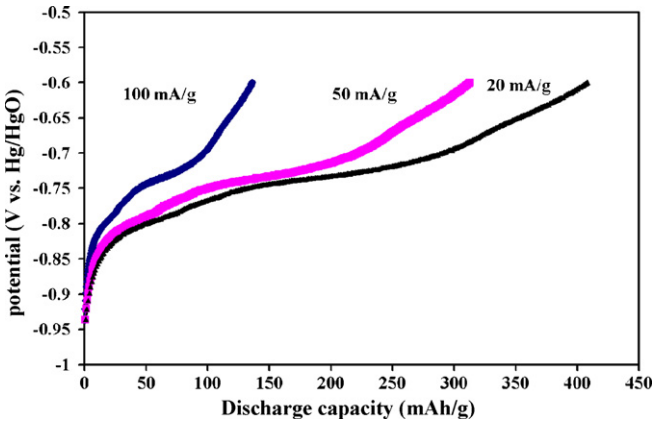

Fig. 7. Galvanostatic discharge curves of nano-Mg_2Ni at different current densities.

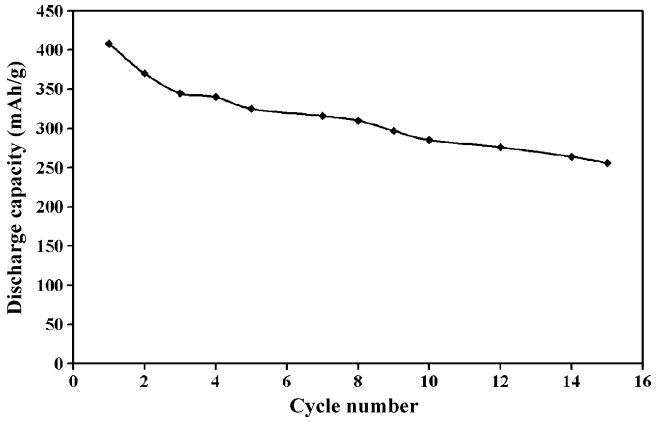

Fig. 8. Cycle test data of the nano-Mg_2Ni.

square technique from the slope and Y intercept of Van't Hoff plots as shown in Fig. 6. The enthalpies and entropies of the Mg_2Ni prepared by polyol reduction and annealing at 573 K were −50.03 kJ/mol, −103.60 J/(mol K) for absorption and 56.35 kJ/mol, 105.36 J/(mol K) for desorption, respectively.

3.2. Electrochemical characteristics

Electrochemical galvanostatic charge/discharge is a more convenient method than a gaseous technique for determining the hydrogen absorption capacity and thermodynamic parameters of a metal hydride at low temperatures. The discharge capacities are calculated from the discharge current and the time required reaching a potential of −0.6 V (Hg/HgO) for Mg_2Ni electrodes, by using the equation:

$$Q_{\text{discharge}} = It \quad (1)$$

The electrode was charged/discharged galvanostatically in 6 M KOH aqueous solution at room temperature. The typical discharge curves at the 1st cycle measured at different discharge current densities are shown in Fig. 7. The discharge capacity decreases with increasing discharge current because of an increase in the over voltage. The maximum discharge capacity obtained was 408 mAh/g at a discharge current density of 20 mA/g in the first cycle. This is much more than that of polycrystalline Mg_2Ni reported previously [3]. The increase in the discharge capacity is due to the formation of nanocrystalline/amorphous alloy by the polyol reduction that improves hydrogenation ability of Mg_2Ni electrode at low temperature because of the hydrogen diffusion in nanocrystalline or amorphous alloy is more facile than the polycrystalline alloy.

Fig. 3 shows discharge capacities at room temperature as a function of cycle number for the Mg_2Ni nanocrystalline alloy prepared by polyol reduction method. The initial discharge capacity was 408 mAh/g at a discharge current density of 20 mA/g. The cycling capacity of polycrystalline Mg_2Ni is low due to the magnesium in Mg_2Ni was easily oxidized in alkaline solution and $Mg(OH)_2$ passive film was formed [15,16]. In order to improve the cyclic stability several modifications like elemental substitution, coating with palladium, nickel and carbon, which will protect the alloy surface have been reported in literature [27]. It was reported that Ni coating is more effective in protection of the surface of the alloy. It can be seen (from Fig. 8) that the decrease in discharge capacity is low. The degradation is about 32% of maximum discharge capacity. This may be because of the coverage of small amount of palladium and nickel nanoparticles on the surface of Mg_2Ni prepared by polyol reduction method, which improves the kinetics of hydrogen diffusion as well as act as function as a protecting layer for the alloy.

The electrochemical pressure–composition isotherms for absorption and desorption of hydrogen were obtained from the equilibrium potential values of the electrodes, measured during intermittent charge and/or discharge cycles at constant current density of 20 mAh/g by using Nernst equation [28]. Fig. 9 shows the pressure–concentration isotherm that is theoretically derived from the equilibrium potential during the electrochemical measurement. The trend of the isotherm is the same as that obtained volumetric measurements. Plateau of the electrochemical isotherm is not flat because of nanocrystalline/amorphous

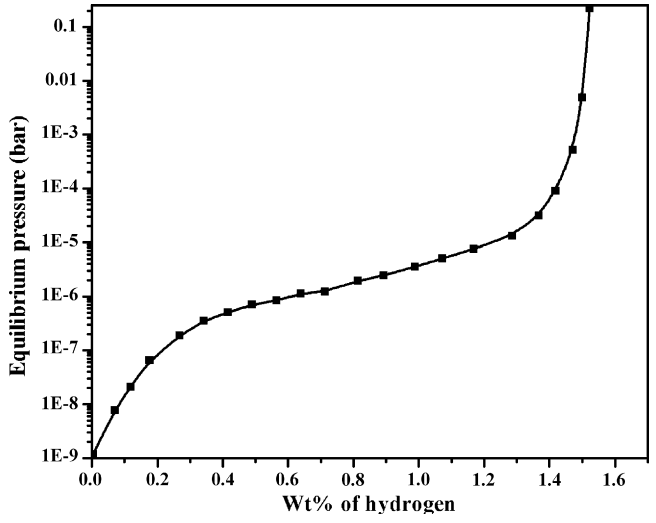

Fig. 9. Electrochemical pressure composition isotherm at a discharge current density of 20 mA/g for the nano-Mg_2Ni alloy.

nature of the material. The maximum absorbed hydrogen amount shown in Fig. 5 is about 1.5 wt%

4. Conclusions

Polyol reduction method is an alternative route to synthesize nanocrystalline/amorphous alloys. Nanosize Mg_2Ni alloy, synthesized by polyol reduction and subsequent annealing at 573 K has shown promising hydrogen absorption as well as electrochemical hydrogen absorption characteristics. The maximum hydrogen storage capacity observed was 3.23 wt% at 603 K. It absorbs 3.2 wt% of hydrogen with in 1 min and desorbs 2.8 wt% of hydrogen with in 15 min at 573 K. The enthalpy and entropy of formation for hydrogen absorption and desorption are −50.03 kJ/mol, −103.60 J/(mol K) for absorption and 56.35 kJ/mol, 105.36 J/(mol K) for desorption, respectively. The maximum discharge capacity was found to be 408 mAh/g at a discharge current density of 20 mA/g. The materials show good stability for number of cycles and degradation was only 32% of maximum discharge capacity after 15 cycles.

References

[1] L. Zaluski, A. Zaluska, J.O. Ström-Olsen, J. Alloys Compd. 217 (1995) 245–249.
[2] U. Köhler, J. Kumpers, M. Ullrich, J. Power Sources 105 (2002) 139–144.
[3] N. Cui, B. Luan, H.K. Liu, J. Power Sources 55 (1995) 263–267.
[4] S. Orimo, H. Fujii, J. Alloys Compd. 232 (1996) L16–L19.
[5] M. Abdellaoui, D. Cracco, A.P. Guegan, J. Alloys Compd. 268 (1998) 233–240.
[6] A.K. Singh, A.K. Singh, O.N. Srivastava, J. Alloys Compd. 227 (1995) 63–68.
[7] C. Suryanarayana, Prog. Mater. Sci. 46 (2001) 1–184.
[8] J. Chen, S.X. Dou, H.K. Liu, J Alloys Compd. 244 (1996) 184–189.
[9] R. Vijay, R. Sundaresan, M.P. Maiya, S.S. Murthy, Int. J. Hydrogen Energy 30 (2005) 501–508.
[10] C. Iwakura, S. Nohara, H. Inoue, Y. Fukumoto, Chem. Commun. (1996) 1831–1832.
[11] T. Kohno, S. Tsuruta, M. Kanda, J. Electrochem. Soc. 143 (1996) L198–L199.
[12] L. Aymard, M. Ichitsubo, K. Uchida, E. Sekreta, F. Ikazaki, J. Alloys Compd. 259 (1997) L5–L8.
[13] D.L. Sun, Y.Q. Lei, W.H. Liu, J.J. Jiang, J. Wu, Q.D. Wang, J. Alloys Compd. 231 (1995) 621–624.
[14] N.H. Goo, J.H. Woo, K.S. Lee, J. Alloys Compd. 288 (1999) 286–293.
[15] W. Liu, Y. Lei, D. Sun, J. Wu, Q. Wang, J. Power Sources 58 (1996) 243–247.
[16] T. Abe, T. Tachikawa, Y. Hatano, K. Watanabe, J. Alloys Compd. 330–332 (2002) 792–795.
[17] T. Kohno, M. Yamamoto, M. Kanda, J. Alloys Compd. 293–295 (1999) 643–647.
[18] R. Janot, L. Aymard, A. Rougier, G.A. Nazri, J.-M. Tarascon, J. Phys. Chem. Solids 65 (2004) 529–534.
[19] Chia-Ming Chen, Jih-Mirn Jehng, Appl. Catal. A: Gen. 267 (2004) 103–110.
[20] Y. Wang, J.W. Ren, K. Deng, L.L. Gui, Y.Q. Tang, Chem. Mater. 12 (2000) 1622–1627.
[21] N. Toshima, Y. Wang, Langmuir 10 (1994) 4574–4580.
[22] B. Jeyadevan, A. Hobo, K. Urakawa, C.N. Chinnasamy, K. Shinoda, K. Tohji, J. Appl. Phys. 93 (2003) 7574–7576.
[23] E. Anil Kumar, M. Prakash Maiya, S. Srinivasa Murthy, Int. J. Hydrogen Energy 32 (2007) 2382–2389.
[24] R. Janot, X. Darok, A. Rougier, L. Aymard, G.A. Nazri, J.-M. Tarascon, J. Alloys Compd. 404–406 (2005) 293–296.
[25] T. Spassov, U. Köster, J. Alloys Compd. 287 (1999) 243–250.
[26] S. Orimo, H. Fujii, Appl. Phys. A 72 (2001) 167–186.
[27] C. Rongeat, M.-H. Grosjean, S. Ruggeri, M. Dehmas, S. Bourlot, S. Marcotte, L. Roue, J. Power Sources 158 (2006) 747–753.
[28] J. Balej, Int. J. Hydrogen Energy 10 (1985) 233–243.